International Journal of Medical, Medicine and Health Sciences
ISSN: 2517-9969
Vol:6, No:5, 2012

Transmit Sub-aperture Optimization in MSTA Ultrasound Imaging Method

YuriyTasinkevych, Ihor Trots, AndrzejNowicki, Marcin Lewandowski

***Abstract*—**The paper presents the optimization problem for the multi-element synthetic transmit aperture method (MSTA) in ultrasound imaging applications. The optimal choice of the transmit aperture size is performed as a trade-off between the lateral resolution, penetration depth and the frame rate. Results of the analysis obtained by a developed optimization algorithm are presented. Maximum penetration depth and the best lateral resolution at given depths are chosen as the optimization criteria. The optimization algorithm was tested using synthetic aperture data of point reflectors simulated by Filed II program for Matlab® for the case of 5MHz 128-element linear transducer array with 0.48 mm pitch are presented. The visualization of experimentally obtained synthetic aperture data of a tissue mimicking phantom and in vitro measurements of the beef liver are also shown. The data were obtained using the SonixTOUCH Research systemequipped with a linear 4MHz 128 element transducerwith 0.3 mm element pitch, 0.28 mm element width and 70% fractional bandwidth was excited by one sine cycle pulse burst of transducer's center frequency.

***Keywords*—**synthetic aperture method, ultrasound imaging, beamforming.

I. Introduction

IN the past decade ultrasound imaging has become one of the preferred diagnostic techniques primarily because of its accessibility, the use of non-ionizing radiation, and real-time display. High resolution ultrasound images are routinely obtained by employing phased array transducers and delay-and-sum beamforming techniques. In this approach, however, the adequate focusing of the examined volume is achieved at the expense of the limited frame rate. Synthetic aperture (SA) methods offer a number of advantages over a conventional beamforming methods based on phased arrays: the higher spatial resolution due to the full dynamic focusing on the transmit and receive, lower power consumption due to the small number of elements used for ultrasound wavefield generation at each transmission and so on. Multi-element Synthetic Transmit Aperture (MSTA) which has been intensively studied recently [1,2] enables increasing the imaging system frame rate providing reasonable compromise between the penetration depth and lateral resolution at the same time. Since in MSTA the transmit aperture comprises several elements, the total transmitted power increases and the signal-to-noise ratio is improved as compared to the conventional synthetic transmit aperture method using a single element in transmit mode. The main concern in the MSTA is a proper choice of the transmit aperture sizeand shift between subsequent emissions. The paper presents the results of theoretical and experimental studies of the developed optimization algorithm, which performs the optimal choice of the number of element in transmit mode using the criteria of maximum penetration depth and lateral resolution at given (different) depths. The optimization is carried out in MATLAB® environment using the Field II [3,4] simulated synthetic aperture data of a system of point reflectors for the case of 5MHz 128-element linear transducer array with 0.48 mm pitch. Experimental results are presented for a tissue mimicking phantom as well as for a beef liver pattern study in vitro.The data were collected using the UltrasonixSonixTOUCH Research system. The results show that the optimal aperture size strongly depends on the required visualization depth. Thus, the best image quality at the low depths (up to 30 mm) can be obtained using 2 element transmit aperture, and for larger depths (60-90 mm) the 4-5 element one is a better choice since it allows to increase the transmitted energy which leads to increase in a signal-to-noise ratio (higher image quality), maintaining lateral resolution at the same time. The paper is organized as follows. In the next section a brief overview of the STA and MSTA methods for ultrasound imaging applications is given. In Sec. 2 the optimization problem for MSTA is stated and the developed algorithm is presented and discussed in details. In Sec. 3 the results of numerical experiments are shown.

The Authorsare with the Institute of Fundamental Technological Research, Polish Academy of Sciences, Warsaw, 02-106, Poland (phone: 4822-8261281; e-mail: yurijtas@ippt.gov.pl).

II. Multi-Element Synthetic Transmit Aperture Method

The MSTA method is a generalization of the conventional synthetic transmit aperture (STA) method which uses a single element in transmit mode. The MSTA instead uses a finite number of elements to transmit unfocused ultrasound wave-field to emulate a single element. This allows to increase the transmit power resulting in improved signal-to-noise ratio and penetration depth. The main advantage of the MSTA is that it provides for the full dynamic focusing both in transmit and receive modes yielding the highest imaging quality. The schematic diagram explaining the MSTA method is sketched in Fig. 1. A full large aperture is synthesized by multiple transmissions. At each time a transmit aperture comprised of several elements is used to emit unfocused wave-field. The

backscattered waves are received by each element independently and the resulting RF echoes are digitized and stored in memory. For an N-element array, and $N_t$elements in transmit mode $N\times M$ independent recordings are required to synthesize a final high resolution image, where M is a number of emissions in one data acquisition cycle. For the case of non-overlapping apertures, which is mainly considered in this paper, M=round(N/N_t). It should be noted, that in the case of overlapping transmit apertures even better image quality can be achieved, but unfortunately the number of transmissions M increases, which leads to the frame rate decrease.

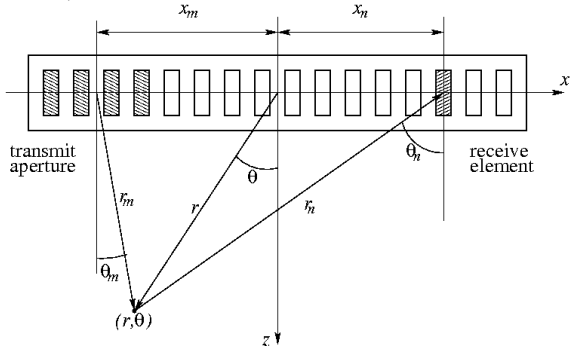

Fig. 1. Transmit and receive elements combination and the focus point in MSTA method.

After finishing the full data acquisition cycle the RF echoes are summed up with properly chosen time delays according to the focus point spatial position (see Fig. 1) in order to synthesize the final high resolution image. Thus, in the case of N-element array for each point in the image, the A-scan signal can be expressed as follows:

$$A_{MSTA}(r,\theta)=\sum_{m=1}^{M}\sum_{n=1}^{N} y_{m,n}\left(\frac{2r}{c}-\tau_{m,n}\right), \qquad (1)$$

where $y_{m,n}(t)$ is the RF echo signal and $\tau_{m,n}$ is the round-trip delay, defined for the (m,n) transmit-receive element combination by the following expression:

$$\tau_{m,n}=\tau_m+\tau_n, \quad 1\le m,n\le N. \qquad (2)$$

The corresponding delays for m^{th} transmit and n^{th} receive elements relative to the imaging point (r,θ) are:

$$\tau_i=\frac{1}{c}\left(r-\sqrt{r^2+x_i^2-2x_i r\sin\theta}\right), \quad i=m,n, \qquad (3)$$

where x_m, x_n are the positions of the m^{th} transmit and n^{th} receive apertures, respectively, and r, θ are the polar coordinates of the imaging point with respect to the origin placed in the center of the transducer's aperture. The frame rate is increased in the MSTA by N_t as compared to the STA method due to decrease of the total number of emissions which speeds up the data acquisition process. Unfortunately, it appears that too excessive increasing of the transmit aperture sizeN_t(and its shift at the same time) leads to the lateral resolution deterioration. However, using a small number of elements in transmit mode allows to increase the system frame rate and provides the best compromise between penetration depth and lateral resolution as compared to the STAmethod. The optimal choice of the transmit aperture size is crucial in the MSTA method. In the next section the corresponding optimization problem is considered for the MSTA algorithm.

III. Transmit Sub-Aperture Optimization

In this section the algorithm for optimal choice of the transmit aperture size in MSTA method is discussed. Here we consider the case of non-overlapping transmit apertures, which means that the shift between subsequent transmissions $N_{sh}=N_t$, N_t being the number of element used in transmit mode. The developed algorithm, however, can be extended to the more general case of the MSTA method with different values of the shift N_{sh}. Usually, $N_{sh}<N_{tr}$yields some improvement of the synthesized image quality at the cost of the frame rate decrease.

In the developed algorithm the maximum penetration depth and best lateral resolution at given depths are chosen as the optimization criteria. A test synthetic aperture data of point reflectors was simulated in Field II program for Matlab® for each size of the transmit aperture. The reflectors are located in the nodes of a rectangular grid. The rows and columns are equidistantly spaced. For each individual experiment the lateral resolution and penetration depth are estimated. The lateral resolution is evaluated for each lateral cross-section coinciding with the rows of the reflectors. In the case of the algorithm presented here only the reflector located at the central column (coinciding with aperture center) is taken into account for simplicity. For convenience the lateral cross-sections are labelled here in accordance with the row numbers of point reflectors.

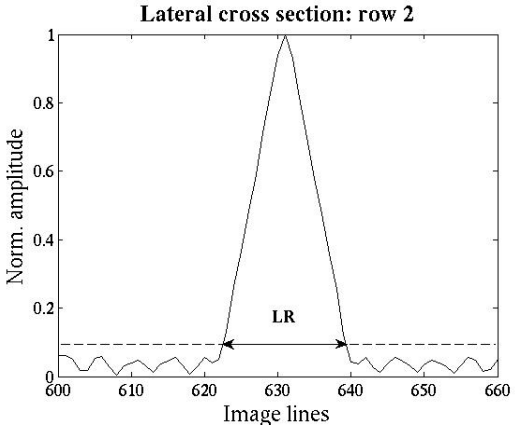

Fig. 2. Evaluation of the lateral resolution for given row: LR is a full width (expressed as a number of image lines) at a given level (0.1 in the considered example) for the reflector located at the intersection of the row and central column of point reflectors.

The lateral resolution in the presented algorithm is estimated by the full width (expressed as a number of image lines) at given level (0.1 in the examples considered in the next section) for the reflector located at an intersection of a given row and the central column of point reflectors (see Fig.

2 for explanation).

The penetration depth is estimated in a similar manner. For the central column of point reflectors the penetration depth is assessed by the relative amplitude of the scattered signal of the deepest "visible" reflector, which means that its normalized (with respect to the maximum value in the considered axial cross-section) amplitude exceeds the given level (0.2 in the examples considered in the next section). This is illustrated in Fig. 3.

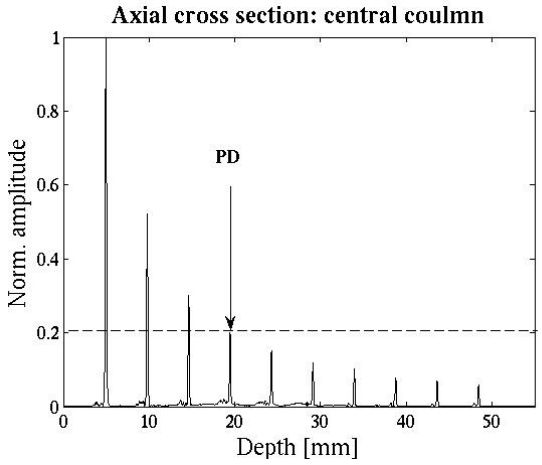

Fig. 3. Evaluation of the penetration depth: PD is the location of deepest reflector for which the normalized amplitude exceeds the given level in the axial cross-section coinciding with the central column of point reflectors.

Below this level the reflectors are assumed to be indistinguishable. In the examples explaining optimization algorithm performance (see Figs. 2, 3) the STA algorithm was exploited for visualization, that is, a single-element was used in transmit mode. For smooth visualization of the lateral cross-sections the interval between subsequent image lines was chosen 0.1 of the transducer pitch (10 image lines per transducer pitch) yielding the total number of 1280 image lines altogether. After estimation of the lateral resolution and penetration depth the optimal system configuration is selected. Two different approaches were realized in the presented algorithm. The first sought for that transmit aperture configuration yielding the maximum penetration depth for lateral resolution being within some tolerance bounds. The second approach, on the other hand, selected the configuration giving the best lateral resolution for penetration depth not less than some minimum acceptable limit.

Let us denote the entire set of all possible aperture configurations with $\boldsymbol{U}$. Its elements – $\boldsymbol{u}$– are described by the parameters:

N_t– transmit aperture width (expressed in number of elements);

N_{sh}– shift of the transmit aperture between subsequent emissions;

PD – penetration depth, achievable by the element (configuration);

LR – lateral resolution, achievable by the element;

FR – frame rate, achievable by the element.

In the following the shorten notation will be adopted in order to describe the element $\boldsymbol{u}(N_t,N_{sh}, PD, LR, FR)$ dependent on the parameters enclosed in brackets. In the further analysis the optimization algorithm operates on the subset $\boldsymbol{U_1}=\{\boldsymbol{u}\in\boldsymbol{U}: N_{sh}=N_t\}$, as was stated above in this section. Using this notation the first optimization approach can be presented as follows.

1. Find the element providing the maximum value of the lateral resolution: LR_{max};
2. Form the subset $\boldsymbol{U_2}=\{\boldsymbol{u}\in\boldsymbol{U_1}: LR>\alpha LR_{max}\}$, comprised of the elements providing the value of the *LR* within certain defined tolerance limit, defined by $0<\alpha<1$;
3. Find the element(s) $\boldsymbol{U_3}=\{\boldsymbol{u}\in\boldsymbol{U_2}: PD=max\{\boldsymbol{u}\in\boldsymbol{U_2}\}\}$, yielding maximum penetration depth
4. Find the element with best *FR* parameter, yielding the optimal choice of the transmit aperture configuration: $\boldsymbol{u}_{\mathbf{opt}}: FR=max\{\boldsymbol{u}\in\boldsymbol{U_3}\}$.

It should be noted that in step 3 several elements can provide the same value of penetration depth, since it is estimated by location of the point reflector, and this location takes discrete values due to the nature of the considered system of point reflectors. It is possible instead to estimate the penetration depth not only using the location of last 'visible reflector', but also taking into account the normalized scattered amplitude associated with it. In this case the step 4 would be superfluous.

The second optimization approach can be presented as follows.

1. Find the element providing the maximum value of the penetration depth: PD_{max};
2. Form the subset $\boldsymbol{U_2}=\{\boldsymbol{u}\in\boldsymbol{U_1}: PD>\beta PD_{max}\}$, comprised of the elements providing the value of the *PD* within certain defined tolerance limit, defined by $0<\beta<1$;
3. Find the element(s) $\boldsymbol{U_3}=\{\boldsymbol{u}\in\boldsymbol{U_2}: LR=max\{\boldsymbol{u}\in\boldsymbol{U_2}\}\}$, yielding maximum lateral resolution
4. Find the element with best *FR* parameter, yielding the optimal choice of the transmit aperture configuration: $\boldsymbol{u}_{\mathbf{opt}}: FR=max\{\boldsymbol{u}\in\boldsymbol{U_3}\}$.

Similarly, as in the first optimization approach, in step 3 several elements can yield the same value of *LR* (it is less likely to happen for larger number of image lines per pitch, which directly follows from the LR definition, see Fig. 2b.). This is due to its discrete nature (defined as a number of image lines, see Fig. 2b). In the example considered further the acceptable decrease in lateral resolution and penetration depth was assumed to be 15% of its maximum values, yielding, accordingly, α=0.85 and β=0.85.

IV. Numerical Results And Discussion

In this section the numerical results illustrating the optimization algorithm performance are presented. A 5MHz 128-element linear transducer with 0.48 mm pitch and 0.15 mm kerf excited by one sine cycle burst pulse is considered.

The Field II simulated synthetic aperture data of the point reflectors discussed in the previous section are used to verify the performance of developed optimization algorithm. The reflectors are placed in the nodes of rectangular grid comprising 10 equidistantly spaced rows and 3 columns. The central vertical line coincides with the transducer aperture centre. The reflectors are spaced 15 mm laterally and 5 mm axially. The MSTA algorithm assuming non-overlaping transmit apertures,$N_{sh}=N_t$,yielding the maximum frame rate increase as compared to the STA, is considered with apodization weights implemented accounting for the transmit and receive aperture angular directivities [2,5].

In Table 1 the optimized values of the transmit aperture width $N_t$are shown for different visualization depths evaluated using different approaches discussed in the previous section. The results of the1st optimization approach correspond to the configuration with maximum penetration depth from within the set of transmit apertures yielding the lateral resolution decrease less than 15% of its maximum value. On the other hand, the 2nd approach presents the configuration which yields the best lateral resolution from the set of transmit apertures for which the penetration depth is not less than 15% of its maximum value. Table I reveals a similarity of the optimal transmit aperture configurations obtained by two different approaches.

TABLE I
OPTIMAL TRANSMIT SUB-APERTURE

D, mm	Approach #1		Approach #2	
	N_t	δLR,%	N_t	δLR,%
5	1	45	1	45
10	1	52	2	32
15	2	22	2	22
20	2	16	3	-
25	3	5	3	5
30	3	12	3	12
35	3	11	4	-
40	4	-	4	-
45	4	-	4	-
50	4	-	4	-

As seen from Table 1 the maximum penetration depth is achieved with N_t=4. For this configuration the decrease in the lateral resolution δLR as compared to the optimized value of N_t at different depths is also shown in Table 1. The best lateral resolution is achieved with STA algorithm using single-element transmit aperture, but only for visualization depths not exceeding 10-15 mm. On the other hand, the configuration with N_t=4 enables visualization of the deepest parts of the phantom, but at the cost of lateral resolution decrease at lower depths in comparison with STA method

In Fig. 4 a 2D ultrasound images of tissue mimicking phantom are shown. Experimental data were acquired by the UltrasonixSonixTOUCH Research system equipped with 4MHz 128 element linear transducer L14-5/38 with0.3 mm element pitch, 0.28 mm element width and 70% fractional bandwidth. The tissue mimicking phantom model 525 Danish Phantom Design with attenuation of background material 0.5 dB/[MHz×cm] was used in the experiments. As seen from Fig. 4 the optimal correlation between penetration depth and lateral resolution is obtained by MSTA-4 with N_t=4 elements in transmit mode. The STA method is characterized by the best lateral resolution at lower depths but has poor penetration depth. Whereas for larger apertures, N_t=8,16, the lateral resolution is worsened and the gain in penetration depth is negligible. To estimate the penetration depth and lateral resolution the axial cross-sections of the image line #1885 (corresponding to the vertical line of reflectors in Fig. 4) and the lateral cross-sections at depths 10 mm and 60 mm of the above phantom for different transmit apertures are shown in Figs. 5 and 6, respectively.

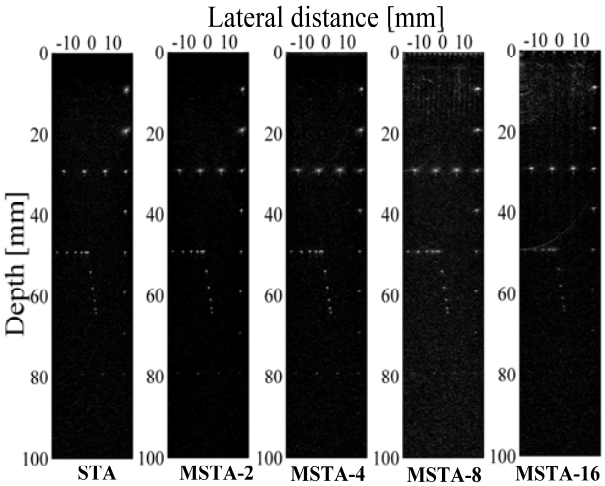

Fig. 4. 2D visualization of tissue mimicking phantom for different transmit aperture size: a single-element aperture – STA and 2,4,8,16-element aperture (MSTA) . All images are displayed over 30 dB dynamic range.

As seen from Fig 5a at the depth of 30 mm the scattered amplitude in the case of MSTA-4 (optimal aperture) is 1.46 and 1.59 times larger than for MSTA-16 (N_t=16) and STA (N_t=1), whereas, from Fig. 5b one can observe that at the depth of 40 mm MSTA-4 yields 1.14 and 2.84 times larger amplitude than MSTA-16 and STA, respectively. The lateral resolution, estimated from the lateral cross-sections at the 0.3 level of its maximum value at different depths is best in the case of STA algorithm, as expected. Thus, at the depth of 10 mm, Fig. 6a, the STA method gives 3% and 20%, and at the depth 60 mm, Fig. 6b, – 3% and 8% better lateral resolution than MSTA-4 and MSTA-16 do, respectively.

In Fig. 7 a 2D ultrasound images of beef liver pattern study in vitro for different transmit aperture size are shown. Data were collected as above using the UltrasonixSonixTOUCH Research system.Fresh beef liver sample was obtained from the local butcher shop within 6–8 hours after slaughter. It was refrigerated until being transferred to the lab.

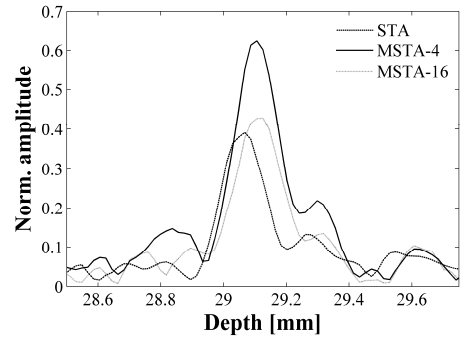

(a)

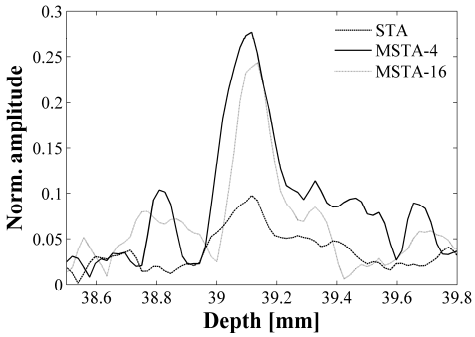

(b)

Fig. 5. Axial cross-sections of the phantom line #1885 at different depths for N_t=1,4,16.

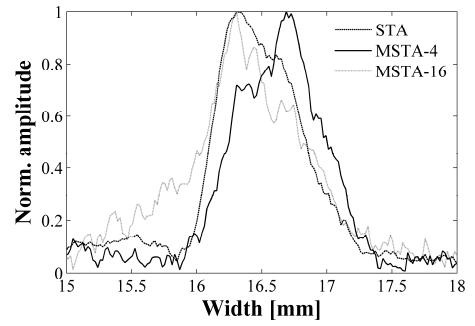

(a)

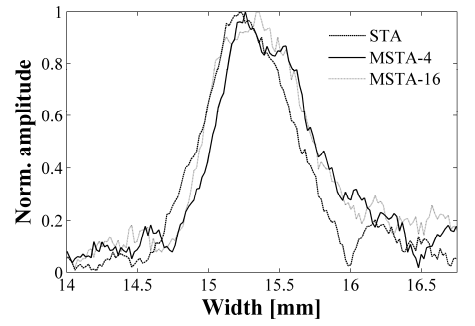

(b)

Fig. 6. Lateral cross-sections at different depths: (a) 10 mm and (b) 60 mm of the reflectors situated on the right hand side of the phantom (see Fig. 4).

Ultrasonic experiments were conducted within 7-9 hours of the removal of the liver from the animal. The bovine liver sample was immersed in water at room temperature during the measurements.

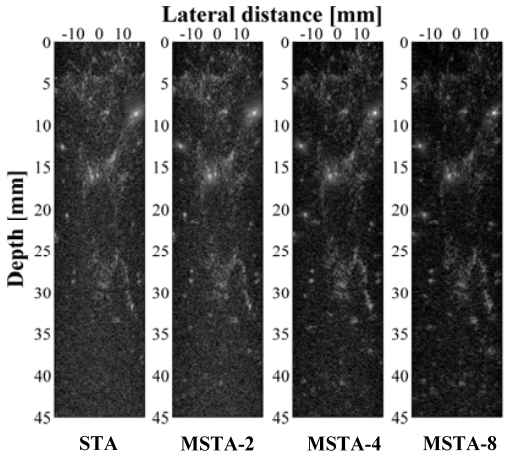

Fig. 7. 2D visualization of beef liver pattern study in vitro for different transmit aperture size for N_t=1,2,4,8. All images are displayed over 50 dB dynamic range.

As seen in Fig. 7 the air bubbles are observed which are almost impossible to avoid in case of in vitro experiments. But here they are helpful for qualitative estimation of the image quality parameters like the lateral resolution and contrast. At the same time the basic liver structure is unchanged in the presented experimental results. As expected, the STA algorithm, using single-element transmit aperture, is characterized by the best image resolution, but the penetration depth is poor. In the case of MSTA-4 with N_t=4 the optimal correlation between resolution and penetration depth can be achieved almost in the entire visualization region. For MSTA with larger aperture, N_t=8, the increase of visualization depth is almost indistinguishable whereas some degradation of image resolution can be observed.

V. Conclusion

The work presents the investigation of the multi-element transmit aperture algorithm (MSTA) for ultrasound imaging. The main concern of the paper is the optimal choice of transmit aperture size providing the best compromise between the lateral resolution and penetration depth of the resulting 2D ultrasound image. For this purpose the corresponding optimization algorithm has been developed. Two different approaches have been implemented and compared which appeared to give similar results. The first one selects the configuration with the best penetration depth and the lateral resolution within some tolerance range, whereas the second one selects the transmit aperture yielding the best lateral resolution for penetration depth not less than some minimum acceptable value. A synthetic aperture data for point reflectorsand 5MHz 128-element linear transducer array excited by a sine cycle simulated in Field II program were used in the numerical examples. For the test phantom the best

image quality as concerns the lateral resolution at low depths of 10-20 mm is achieved by the small apertures with N_t=1,2. On the other hand, the deeper phantom regions are better visualized if the transmit aperture width N_t=4 is selected. The developed algorithm performance was tested using synthetic aperture data obtained from experimental measurements. For this purpose the UltrasonixSonixTOUCH Research system equipped with 4MHz 128 element linear transducer L14-5/38 with0.3 mm element pitch, 0.28 mm element width and 70% fractional bandwidth was used. The visualizations of tissue mimicking phantom and beef liver pattern study in vitro have shown that, as expected, MSTA algorithm with N_t=4 gives optimal correlation between lateral resolution and penetration depth, yielding good image quality and reasonable frame rate increase in comparison to the STA method. In this paper the MSTA algorithm with transmit aperture shift equal to its size was mainly considered. However, the case with $N_{sh}<N_t$, which is characterized by somewhat better imaging quality but worse frame rate as compared to $N_{sh}=N_t$, can be also treated by the approach. This, however, requires some modification of the optimization criteria and is a problem for future study.

Acknowledgment

This work was supported by the Polish Ministry of Science and Higher Education (Grant NN518418436).

References

[1] K. L. Gammelmark, J. A. Jensen, Multielement synthetic transmit aperture imaging using temporal encoding, IEEE Trans. Medical Imaging, 22, (4), 552-563, 2003.

[2] I. Trots A. Nowicki, M. Lewandowski, Y. Tasinkevych, Multi-element synthetic transmit aperture in medical ultrasound imaging. Archives of Acoustics, 35 (4), 687–699, 2010.

[3] J. A. Jensen, Field: A Program for Simulating Ultrasound Systems. 10th Nordic-Baltic Conference on Biomedical Imaging Published in Medical & Biological Engineering & Computing, 34, Supplement 1, Part 1, 351-353, 1996.

[4] J. A. Jensen, N. B. Svendsen, Calculation of pressure fields from arbitrarily shaped, apodized, and excited ultrasound transducers. IEEE Trans. Ultrason., Ferroelec., Freq. Contr., 39, 262-267, 1992.

[5] Y.Tasinkevych, I. Trots, A. Nowicki, P. A. Lewin, „Modified synthetic transmit aperture algorithm for ultrasound imaging," Ultrasonics, 52 (2), 333-342, 2012.